

# Debris elimination in a droplet-target laser-plasma soft x-ray source

L. Rymell and H. M. Hertz

Lund Institute of Technology, Department of Physics, P.O. Box 118, S-221 00 Lund, Sweden

(Received 28 December 1994; accepted for publication 22 June 1995)

A tabletop high-brightness line-emitting laser-plasma soft x-ray source utilizing single microscopic droplets as target is shown to produce several orders of magnitude less debris than conventional-target sources. Quantitative measurements of debris deposition rates and x-ray flux at different directions around the droplet plasma are presented. With ethanol droplets and a 10 Hz, 70 mJ/pulse laser, typically  $\sim 1 \times 10^{12}$  photons/(sr·pulse·line) are emitted from the C V and C VI lines in the water window. The debris deposition is further reduced with a small, localized gas jet shield, which is transparent to the x-rays. The deposition rate through the gas shield has been determined to be  $\sim 0.2$  pg/(sr·pulse). Thus, this droplet-target laser-plasma x-ray source is four orders-of-magnitude cleaner than a low-debris plastic tape target laser plasma of similar brightness, making it useful for x-ray microscopy and lithography. © 1995 American Institute of Physics.

## I. INTRODUCTION

The laser-plasma is an attractive source for x-ray microscopy and lithography due to its high brightness, high spatial stability, and relatively low cost.<sup>1</sup> A disadvantage is the emission of debris, which may damage components in the vicinity of the plasma. Using small droplets as a laser-plasma target, debris production is reduced by several orders of magnitude.<sup>2</sup> In the present article, the magnitude and angular dependence of the droplet-target debris production is quantitatively analyzed and a microscopic localized gas jet shield is shown to practically eliminate the effect of the residual debris from the x-ray source.

Conventionally, laser-plasma x-ray sources use solid targets.<sup>1,3</sup> With laser intensities around  $10^{13}$ – $10^{14}$  W/cm<sup>2</sup>, such soft x-ray sources may reach conversion efficiencies of several tens of percents.<sup>4</sup> Unfortunately, using solid targets, laser plasmas eject significant amounts of debris, i.e., atoms, ions, and particles, which may damage and coat fragile x-ray optics and other components positioned close to the plasma. A short distance between the plasma and the component is important to increase the useful x-ray flux since the plasma is an incoherent x-ray source. Several methods have been invented to reduce the effect of debris, e.g., using a backing pressure of noble gases,<sup>5–8</sup> a fast shutter system that eliminates part of the debris,<sup>8,9</sup> or a toroidal relay mirror for the protection of sensitive components.<sup>10</sup> Experimental attempts to minimize the production of debris include thin film tape targets<sup>7,9,11</sup> that reduce the amount of emitted debris by avoiding chock wave ejection or delayed evaporation. Still, significant amounts of debris particles are produced, presumably from cooler zones of the target, which are illuminated by the lower-intensity radial wings of the beam. Thus, it would be preferable to use a small target, such as a microscopic droplet, which has no target material at the edges of the beam. Furthermore, when the small mass of the droplet is exposed only to the high-intensity central part of the laser beam, a very large fraction of the atoms in the droplet are highly ionized and emit x-rays, thereby significantly reducing the ionic and atomic debris production for a given x-ray flux. We have previously demonstrated qualitatively that

with  $\sim 10$   $\mu$ m ethanol droplets, debris production is reduced by nearly three orders of magnitude compared to a plastic tape target without reduction of x-ray brightness.<sup>2</sup> Below, quantitative measurements of the debris emission and the soft x-ray flux at different directions from this droplet plasma are presented. The measurements are compared with quantitative debris determinations performed on laser plasmas using solid metal targets,<sup>5,6,8,12</sup> metal tape targets,<sup>7</sup> and a thin film plastic tape target. Quantitative measurements of debris have been performed with several methods, e.g., optical absorption,<sup>6,8,12</sup> reflectivity,<sup>7</sup> chemical assay,<sup>5,12</sup> and atomic force microscopy.<sup>13</sup> An alternative implementation of a low-debris x-ray source based on a small mass target is proposed and theoretically investigated in Ref. 14.

We also present a new method that reduces the effect of the minute residual debris from the droplet source to negligible levels. By positioning a small capillary nozzle with a gas flow of, e.g., nitrogen, in front of the sensitive component to be protected, we achieve a localized gas shield that efficiently reduces the residual debris deposition by approximately 30 times. This debris shield has several advantages compared to methods using a backing pressure in the vacuum tank<sup>5,6,7,8</sup> since comparatively high gas densities can be achieved over small distances. Due to the high density and localized nature of the gas shield, components may be protected even if they are positioned close to the plasma, resulting in higher x-ray flux. Furthermore, breakdown in the laser beam prior to the focus is avoided since the local high gas density does not affect the target area. Finally, the gas flow is sufficiently low to be compatible with small-scale vacuum pumps.

## II. EXPERIMENTS

The schematic experimental arrangement of the droplet-target laser-plasma x-ray source is shown in Fig. 1. It is briefly described below and more details are given in Ref. 2. The target for the x-ray source is 10–15  $\mu$ m diameter ethanol droplets, which are produced by a  $\sim 1$  MHz piezoelectrically vibrated capillary glass nozzle in an  $\sim 1 \times 10^{-4}$  mbar pressure vacuum tank. The  $\sim 10$   $\mu$ m diameter capillary

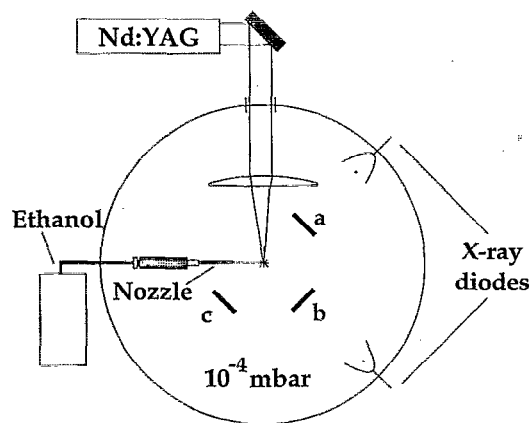


FIG. 1. Experimental arrangement for measurements of the debris deposition rate from the laser-plasma droplet x-ray source.

nozzle generates a spatially stable train of equally sized and equally spaced droplets at a rate of  $\sim 10^6$  drops/s with a droplet velocity of  $\sim 50$  m/s.<sup>15</sup> The beam from a frequency doubled, 10 Hz active/active/passive modelocked Nd:YAG laser (Continuum PY61C-10) is focused with a 50 mm lens onto the droplets, resulting in a focal spot diameter of approximately  $12 \mu\text{m}$ . Due to the high speed of the droplets combined with the small focal volume, accurate temporal triggering of the laser pulse is necessary for a single laser pulse to hit a single target droplet. Thus, the  $\pm 30$  ns laser jitter results in a  $\pm 1.5 \mu\text{m}$  spatial variation of the droplet position in the focal volume. The energy of each  $\sim 130$  ps long pulse is 70 mJ at  $\lambda = 532$  nm, resulting in approximately  $4 \times 10^{14}$  W/cm<sup>2</sup> in the focus. The temporal shape of the laser pulse is practically Gaussian as measured with a streak camera. The contrast ratio between the main pulse and pre- or afterpulses stemming from the original modelocked pulse train is  $> 1000:1$ . This arrangement is a high-brightness soft x-ray source in the  $\lambda = 1.5\text{--}4$  nm range, emitting narrow-band line radiation from C V, C VI, O VII, and O VIII in combination with a very low broadband background.<sup>2</sup> Emission at longer wavelengths ( $\lambda = 10\text{--}20$  nm) has also been characterized.<sup>16</sup>

The x-ray flux from the source was determined by measuring the time integrated signal from an x-ray diode (Hamamatsu G-1127-02) covered by a 170/100 nm Ag/Al sandwiched soft x-ray filter.<sup>2</sup> This filter primarily transmits the  $\lambda = 3.37, 3.50,$  and  $4.03$  nm C V and C VI lines. Given the relative intensities of the lines determined by a grazing incidence monochromator, it was deduced that the flux from the strongest lines (C VI at  $\lambda = 3.37$  nm) is  $\sim 1 \times 10^{12}$  photons/(sr·line·pulse) at  $45^\circ$  angle to the incident laser beam. More than 50% of the photons are emitted from a  $< 15 \mu\text{m}$  kernel, as measured by a pinhole camera. Thus, the integrated spectral brightness of the line is  $> 0.1 \mu\text{J}/(\text{sr} \cdot \mu\text{m}^2 \cdot \text{pulse})$ .

For initial characterization of the emitted debris, carefully cleaned glass slides were positioned in the vacuum chamber close (typically 20 mm) to the laser plasma. Figure 1 shows three different positions. The slides were “exposed” to debris for up to 18 h of continuous 10 Hz operation. The deposited layer was then investigated with x-ray photoelec-

tron spectroscopy (XPS). The XPS measurements show that the layer consists practically solely of carbon.

In order to determine the thickness of the debris layer quantitatively, and thus, the debris deposition rate, two methods were used. The first was angle-resolved x-ray photoelectron spectroscopy (ARXPS).<sup>17</sup> For these measurements, a glass slide was coated with a thin layer of gold ( $\sim 150$  nm) and positioned at an angle of  $45^\circ$  to the incident laser beam 20 mm from the laser plasma (position a in Fig. 1) during 3 h of 10 Hz operation. The glass slide was then mounted in the XPS apparatus (Kratos) and exposed to 1.25 keV x-rays. The intensity of the 4p and 4f gold photo electrons, which were emitted through the deposited debris layer, was then measured at different angles. The intensity  $I$  of the photoelectron emission is<sup>17</sup>

$$I = C(\theta) I_0 e^{-x/\lambda \sin \theta}, \quad (1)$$

where  $I_0$  is the intensity from a clean gold layer,  $\lambda$  is the electron attenuation lengths<sup>18</sup> for the gold electrons in the debris layer,  $\theta$  is the emission angle measured with respect to the surface plane,  $x$  is the thickness of the deposited debris layer, and the factor  $C(\theta)$  is discussed below. To compensate for the larger area of the slide subtended by the field of view of the electron detection system at larger angles and experimental artifacts [the factor  $C(\theta)$  in Eq. (1)], we used the 1s carbon signal to normalize the gold signals. The deposited debris layer was determined to be  $0.8 \pm 0.4$  nm thick. Assuming that the density of the deposited debris layer is  $2 \text{ g/cm}^3$  (amorphous carbon), this corresponds to a deposition rate of  $6 \pm 3 \text{ pg}/(\text{sr} \cdot \text{pulse})$ . These ARXPS results agree well with results obtained from the second method, optical absorption measurements. In this case, the debris deposition was performed in the same way as for the ARXPS measurements, differing only in that nongold-coated glass slides were used. The absorption in the layer was measured with a HeNe laser and lock-in detection. On each slide a small reference area was protected from debris deposition so that the attenuation due to clean surface reflection could be measured. In order to avoid influence of thermal drifts on the measurement accuracy, each absorption measurement consisted of sequential transmission measurements of the debris and reference areas. Typically, six such absorption measurements were averaged, resulting in a minimum detectable absorption of 0.05% due to noise. The absorption measurements were calibrated to absolute thickness by measuring the absorption of reference glass slides with a nominal carbon surface mass density of  $4.9 \mu\text{g/cm}^2$ .<sup>19</sup> XPS measurements of the reference slides and the debris slides result in the same atomic abundancies. Although the deposition on the reference slides was performed by a different method, these slides look very similar to the debris-deposited slides upon inspection in an optical microscope.

The major advantage of the optical absorption method is that it makes measurements of very thin layers possible, thus reducing the debris exposure time. The detectable absorption of 0.05% corresponds to a minimum measurable surface mass density of  $3.6 \text{ ng/cm}^2$  (i.e., 0.018 nm thickness for a

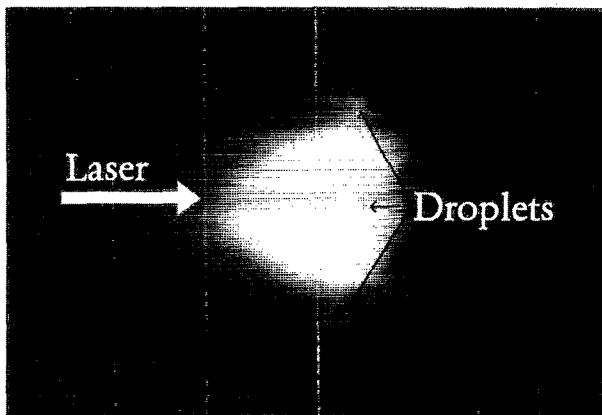


FIG. 2. Photographic recording of the visible ( $\lambda > 590$  nm) emission from a droplet-target plasma. Note the asymmetric plasma cloud and the neighbor droplets on each side of the target droplet.

density of  $2 \text{ g/cm}^3$ ). For such thin layers, the ARXPS data are too noisy to provide sufficient accuracy. The optical absorption measurements resulted in a deposition rate at a  $45^\circ$  angle to the incident beam of  $6.2 \text{ pg}/(\text{sr}\cdot\text{pulse})$ , which is in good agreement with the ARXPS measurements. Within the limit due to the spatial resolution of the absorption measurements (approximately  $200 \mu\text{m}$ ), the deposited layer is uniform. For comparison, the debris deposition rate was measured from a conventional low-debris thin ( $12 \mu\text{m}$ ) cassette plastic tape target,<sup>9</sup> resulting in  $5 \text{ ng}/(\text{sr}\cdot\text{pulse})$  at  $45^\circ$ . XPS studies show a close resemblance between the deposited tape target and the droplet target films. Also in optical inspection, the two films look similar, except for the existence of larger debris particles in the tape-target measurements. The x-ray flux from the tape target is similar to that of the droplet target.

Several investigators have found that the debris deposition is not necessarily uniformly distributed in space.<sup>6,8,12</sup> This is also true for the laser-plasma droplet source. The deposition rate at  $135^\circ$  and  $225^\circ$  angles to the incident beam (position b and c in Fig. 1) was  $3.8\text{--}4.6 \text{ pg}/(\text{sr}\cdot\text{pulse})$ , i.e.  $\sim 70\%$  of the deposition rate at a  $45^\circ$  angle. The fact that more debris is emitted backwards towards the incident beam is also supported by photographs of the plasma. In Fig. 2 the visible emission from the plasma indicates that the plasma plume is asymmetric and a larger part propagates towards the incident laser beam. The photograph is taken through a colored glass filter (OG590), in order to eliminate the scattered laser light. These deposition results are interesting since the soft x-ray flux at a  $135^\circ$  angle was determined to be  $\sim 1.5 \times 10^{12} \text{ photons}/(\text{sr}\cdot\text{line}\cdot\text{pulse})$ , i.e.,  $\sim 50\%$  higher than the ones reported for  $45^\circ$ . The angular dependence of the debris emission and x-ray flux is discussed in Sec. III.

Due to the small size of the target droplet, the entire droplet is exposed to the high-intensity central parts of the focused laser beam. Thus, there is no target material in the low-intensity Gaussian tails of the beam. Therefore we assume that nearly all debris material emitted from the target is in the form of ions or very small fragments. This assumption is supported by the higher degree of ionization observed in spectra from the droplet target compared to spectra recorded with a plastic tape target,<sup>16</sup> the absence of observable larger

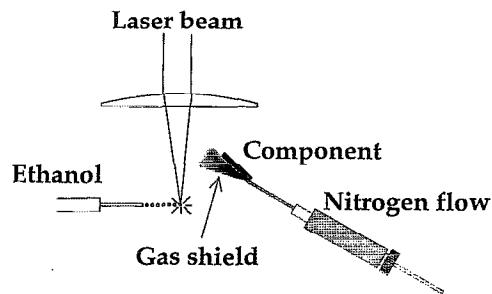


FIG. 3. Experimental arrangement for the localized gas jet debris shield.

debris particles on the glass slides, and the absence of debris-induced pinholes in free-standing thin ( $< 100 \text{ nm}$ ) metal foils positioned close to the plasma. This fact makes the laser-plasma droplet target suitable to be combined with a new debris-shielding technique using a localized miniature gas jet, since only few collisions between the gas molecules and such small debris fragments are needed to provide sufficient momentum transfer to slow down and stop the fragments. The experimental arrangement for the gas jet debris shield is shown in Fig. 3. A capillary nozzle was positioned in close proximity to a glass slide  $20 \text{ mm}$  from the plasma at a  $45^\circ$  angle to the laser beam. A continuous nitrogen gas flow with an initial pressure of  $\sim 40$  bars was forced through the  $\sim 10 \mu\text{m}$  diameter glass nozzle. This created a cone of gas in front of the glass slide. The  $10 \text{ Hz}$  plasma source was operated for  $5 \text{ h}$  in order to record a measurable debris layer. The glass slide was then investigated using the optical absorption method resulting in a deposition rate of  $\sim 0.2 \text{ pg}/(\text{sr}\cdot\text{pulse})$ . This is approximately 30 times less than the values obtained without the localized gas jet debris shield. The debris deposition was reduced to these levels on an area of a few  $\text{mm}^2$  centered  $1\text{--}2 \text{ mm}$  in front of the nozzle tip. The soft x-ray transmission through the nitrogen gas shield was measured at two wavelengths in the water window:  $2.85 \text{ nm}$  (C VI  $1s\text{--}3p$ ), which is below the K absorption edge for nitrogen, and  $3.37 \text{ nm}$  (C VI  $1s\text{--}2p$ ), which is above the edge. Within the  $3\%$  noise in such measurements, no absorption was observed at any of the wavelengths.

### III. DISCUSSION

The measured debris deposition rates compare favorably to similar measurements on conventional targets. To summarize, the deposition rate from the unshielded droplet target source in  $1 \times 10^4$  mbar vacuum was found to be  $\sim 6 \text{ pg}/(\text{sr}\cdot\text{pulse})$  at  $45^\circ$  and  $\sim 4 \text{ pg}/(\text{sr}\cdot\text{pulse})$  at  $135^\circ$  and  $225^\circ$  angles to the incident beam. With the localized gas jet debris shield a deposition rate of  $\sim 0.2 \text{ pg}/(\text{sr}\cdot\text{pulse})$  was measured at  $45^\circ$ . Comparison measurements on the tape-target showed a deposition rate of  $\sim 5 \text{ ng}/(\text{sr}\cdot\text{pulse})$  at  $45^\circ$  with no backing pressure. Thus, the debris deposition rate of the unshielded droplet source is approximately three orders of magnitude less than that of a comparable conventional low-debris target. With the localized gas jet the deposition is more than four orders of magnitude less. The debris deposition rates of the droplet target source also compare well with quantitative

debris measurements performed by other investigators in Refs. 5,6,7,8,12. Using various metals, configured both as solid and tape targets, these authors typically measure debris deposition rates on the order of 1–20 ng/(sr·pulse) without backing pressure and an order of magnitude less with backing pressure. At certain angles less debris is recorded. Although a direct comparison is not possible since these quantitative measurements typically have been performed with different laser systems than ours and on metal targets, the significant reduction of debris using the droplet target is illustrated.

Our debris deposition rate measurements are expected to be correct within a factor of 2. The uncertainty in the ARXPS layer thickness determination is typically  $\pm 50\%$  due to the spread in the literature data on the electron attenuation length and noise in the inversion calculation. In addition, the accuracy is reduced due to the uncertainty in the density ( $2 \pm 0.2 \text{ g/cm}^3$ ) of the deposited layer. The optical absorption measurements are assumed to be correct to within 30%, which is mainly due to the calibration procedure. Noise is due to the 0.05% minimum detection limit, which corresponds to a minimum measurable deposition rate of, e.g.,  $< 0.1 \text{ pg/(sr}\cdot\text{pulse)}$  after 5 h of 10 Hz operation 20 mm from the source. Finally, it should be mentioned that the estimated accuracy in the x-ray flux measurements is  $\pm 50\%$ , which is primarily due to uncertainty in the sensitivity of the x-ray diode.<sup>2</sup>

The significant reduction of larger debris particles from the droplet x-ray source allows the use of new methods to eliminate the residual debris. An electric field trap would efficiently remove ions and small charged fragments, but atomic and uncharged particulate debris remain unaffected. Furthermore, in order to obtain a reasonable debris collection efficiency in combination with a short distance between the source and the object, high electric fields have to be applied close to the target. Due to the emitted ions, this often results in electrical breakdown problems in the high-voltage trap. Alternatively, thin film soft x-ray windows may be used to protect fragile components. These intercept atomic and ionic debris and the lack of larger particles emitted from the droplet source increase their lifetime compared to when used with conventional targets. However, such windows always exhibit some x-ray absorption which reduces the x-ray flux. Furthermore, there is a long-term degradation of the x-ray transmission due to deposition by the residual debris from the droplet source. The gas jet debris shield described here does not experience such long-term degradation due to the continuous gas flow, is highly transparent to the x-rays, and removes both charged and uncharged debris. This debris shield is a localized version of the well-known debris reduction method using a backing pressure in the chamber. However, using a backing pressure in combination with conventional targets, which produce more and larger debris particles, requires long distances and/or high pressures to reduce the debris deposition rate. Thus, the transmission of x-rays may be effected. Furthermore, a larger source-component distance reduces the useful soft x-ray photon flux since the plasma is an incoherent x-ray source. Finally, a high pressure at the target increases the probability of laser breakdown prior to the target,

resulting in that a lower laser intensity may have to be used. By using the localized gas jet shield in combination with the droplet target we eliminate these disadvantages. As shown above, transmission of the desired wavelengths is unaffected in our arrangement even if we use nitrogen, which exhibits absorption edges in the wavelength region of interest. The reason for this is that the density in the gas jet decreases rapidly with distance from the nozzle. Alternatively, nozzles with a slightly larger diameter could probably be used to spectrally filter the emitted radiation. Even if the gas density decreases very rapidly as a function of distance from the nozzle tip, the mean free path for a debris ion or small fragment in our gas jet is sufficiently short to efficiently stop the debris even a few millimeters from the nozzle.

The fact that the droplet target plasma is emitting less debris and higher soft x-ray flux on the rear face of the droplet may be caused by additional focusing of the incident laser beam in the transparent droplet, which acts as a microscopic lens.<sup>20</sup> Thus, the plasma formation is initiated by the leading edge of the laser pulse at the focus, which is located just outside the rear face of the droplet. The initiation would then occur in the evaporated gas cloud surrounding the droplet. As the Gaussian laser pulse reaches its temporal intensity maximum, the plasma wave propagates towards the laser beam, which heats the plasma and the droplet. Since nearly all target material is on the side of the incident beam, a majority of the debris is emitted toward the beam.

Although the most important property of the laser-plasma droplet-target source is the three orders-of-magnitude reduction of debris, the source has many other advantages compared to conventional laser-plasma targets, such as bulk metals or low-debris thin films. It has high brightness, produces line emission soft x-ray radiation suitable for, e.g., zone plate x-ray optics, provide fresh target drops for full-day operation without interrupts, allows high operating frequency (up to MHz), and provides excellent geometric access. There are many applications of this type of laser-plasma x-ray source. The primary objective of our work is to develop a tabletop source for x-ray microscopy and proximity lithography. For this purpose soft x-ray emission in or just below the water window ( $\lambda = 2.3\text{--}4.4 \text{ nm}$ ) is important. In the microscopy case, protection of, e.g., fragile zone plate optics is essential. The localized gas jet shield is useful for such small components. For the lithography, where production requires long-term operation between stops, the three-to-four orders-of-magnitude reduction in debris flux in combination with uninterrupted target operation at high operating frequency is equally important. The significant emission around  $\lambda = 13 \text{ nm}$ <sup>16</sup> may prove valuable for projection lithography as well. Due to the flexibility of the drop formation method, the target material is not restricted to the ethanol used in this study, but can be used for a vast number of liquids or solutions. Thus, new wavelengths may be generated,<sup>21</sup> making the droplet target a versatile x-ray source for many applications. Furthermore, we expect that the debris deposition rates will be further reduced when liquids containing only gaseous compounds (e.g., water) are used.

## ACKNOWLEDGMENTS

The authors gratefully acknowledge Lars T. Anderson and Ingolf Lindau, for XPS assistance and discussions, Terje Rye, at Siemens-Elcoma, who provided them with the capillary nozzles, and Lars Malmqvist, Magnus Berglund, and Lars Engström for valuable discussions. This work was financed by the Swedish Natural Science Research Council, the Swedish Research Council for Engineering Sciences, the Swedish Board for Technical Development, and the Wallenberg Foundation.

<sup>1</sup>See, e.g., several articles in *X-Ray Microscopy III*, edited by A. G. Michette, G. R. Morrison, and C. J. Buckley (Springer, Berlin, 1992); M. Kühne and H.-C. Petzold, *Appl. Opt.* **27**, 3926 (1988).

<sup>2</sup>L. Rymell and H. M. Hertz, *Opt. Commun.* **103**, 105 (1993).

<sup>3</sup>R. Kaufmann, in *Handbook of Plasma Physics*, edited by M. N. Rosenbluth and R. Z. Sagdeev (North Holland, Amsterdam, 1991), Vol 3; D. J. Nagel, C. M. Brown, M. C. Peckerar, M. L. Ginter, J. A. Robinson, T. J. McIlrath, and P. K. Carroll, *Appl. Opt.* **23**, 1428 (1984).

<sup>4</sup>R. Kodama, K. Okada, N. Ikeda, M. Mineo, K. A. Tanaka, T. Mochizuki, and C. Yamanaka, *J. Appl. Phys.* **59**, 3050 (1986).

<sup>5</sup>M. L. Ginter and T. J. McIlrath, *Appl. Opt.* **27**, 885 (1988).

<sup>6</sup>F. Bijkerk, E. Louis, M. J. van der Wiel, I. C. E. Turcu, G. Tallents, and D. Batani, *J. X-Ray Sci. Technol.* **3**, 133 (1992).

<sup>7</sup>L. Shmaenok, F. Bijkerk, E. Louis, A. van Honk, M. J. van der Wiel, Yu. Platonov, A. Shevelko, A. Mitrofanov, H. Frowein, B. Nicolaus, F. Voss, and D. Désor, *Microelectron Eng.* **23**, 211 (1994).

<sup>8</sup>M. Richardson, W. T. Silfvast, H. A. Bender, A. Hanzo, V. P. Yanovsky, F. Jin, and J. Thorpe, *Appl. Opt.* **32**, 6901 (1993).

<sup>9</sup>M. S. Schulz, A. G. Michette, and R. E. Burge, in Ref. 1, p. 58.

<sup>10</sup>R. J. Rosser, R. Feder, A. Ag, F. Adams, P. Celliers, and R. J. Speer, *Appl. Opt.* **26**, 4313 (1987).

<sup>11</sup>S. J. Haney, K. W. Berger, G. L. Kubiak, P. D. Rockett, and J. Hunter, *Appl. Opt.* **32**, 6934 (1993).

<sup>12</sup>J. A. Trail, Ph.D. thesis, Stanford University, 1989.

<sup>13</sup>K. Gabel, M. Richardson, M. Kado, and A. Vassiliev, *Opt. Lett.* **19**, 2047 (1994).

<sup>14</sup>M. Richardson, K. Gabel, F. Jin, and W. T. Silfvast, *Soft X-Ray Projection Lithography*, edited by A. M. Hawryluk and R. H. Stulen (Optical Society of America, Washington, DC, 1993), p. 156.

<sup>15</sup>J. Heinzl and C. H. Hertz, *Adv. Electron. Electron Phys.* **65**, 91 (1985).

<sup>16</sup>L. Rymell, H. M. Hertz, and L. Engström, in *Proc. X-ray Microscopy IV*, edited by A. I. Erko and V. V. Aristov (Chernogolovka, Russia, in press).

<sup>17</sup>J. E. Fulgham, *Surf. Interface Anal.* **20**, 161 (1993).

<sup>18</sup>I. Lindau and W. E. Spicer, *J. Electron Spectrosc. Relat. Phenom.* **3**, 409 (1994).

<sup>19</sup>Arizona Carbon Foil Co., Tuscon, AZ.

<sup>20</sup>R. K. Chang, J. H. Eickmans, W.-F. Hsieh, C. F. Wood, J.-Z. Zhang, and J.-B. Zheng, *Appl. Opt.* **27**, 2377 (1988).

<sup>21</sup>L. Rymell, M. Berglund, and H. M. Hertz, *Appl. Phys. Lett.* **66**, 2625 (1995).